Available online at www.sciencedirect.com
ScienceDirect
Journal of the European Ceramic Society 28 (2008) 1809–1814
www.elsevier.com/locate/jeurceramsoc

# Neutron diffraction residual stress analysis of zirconia toughened alumina (ZTA) composites

J.F. Bartolomé [a], G. Bruno [b,*], A.H. DeAza [c]

[a] *Instituto de Ciencia de Materiales de Madrid, Consejo Superior de Investigaciones Científicas (CSIC), C/ Sor Juana Inés de la Cruz, 3, 28049 Madrid, Spain*
[b] *School of Materials, Manchester Materials Science Centre, Grosvenor Street, Manchester, M1 7HS, UK*
[c] *Instituto de Ceramica y Vidrio, CSIC, C/ Kelsen 5, 28049 Madrid, Spain*

Received 30 June 2007; received in revised form 17 December 2007; accepted 20 December 2007
Available online 11 March 2008

**Abstract**

Measurements of the residual stresses in zirconia toughened alumina (ZTA) composites, containing 1.7, 14 and 22 vol% yttria-stabilized zirconia (3Y–TZP) were obtained by neutron diffraction. Over the range of volume fraction investigated, the hydrostatic stress in alumina and zirconia phases varies roughly linearly with the zirconia content. It is shown that these features can be qualitatively understood by taking into consideration the thermal expansion mismatch between the $ZrO_2$ and $Al_2O_3$ grains. In addition, a decrease of the $Al_2O_3$ line broadening is observed, which implies a decreasing micro-residual strain due to the $ZrO_2$ particles in the alumina. It is inferred that the residual strain field is highly hydrostatic, and that a decrease of the grain boundary shear stress occurs as a function of the reinforcement volume fraction. This phenomenon is more important in the case of 1.7 vol% zirconia composite because the zirconia particles are in the nanometre size range, with a narrow distribution.


*Keywords:* Ceramic-matrix composites (CMCs); Zirconia Toughened Alumina (ZTA); Residual stress; Neutron diffraction

## 1. Introduction

Internal stresses in discontinuously reinforced ceramic–ceramic composites mainly arise on cooling from fabrication temperature, owing to the thermo-elastic mismatch between their constituents.[1] Substantial strains may be generated in alumina matrix ceramics by including zirconia second-phase particles, the material being known as zirconia toughened alumina (ZTA). The linear thermal expansion coefficient (CTE) of the alumina matrix is $\alpha_{Al_2O_3} = 8 \times 10^{-6}\,^{\circ}C$ while that of the zirconia particles is $\alpha_{ZrO_2} = 12 \times 10^{-6}\,^{\circ}C$. When this composite is cooled from the sintering temperature, the reinforcement contracts more than the matrix. This results in tensile stress in the particles and compressive stress in the matrix. Since the reinforcement particles have a nearly spherical form, the mean field stress is generally hydrostatic. However, simulation works[2,3] have shown that the residual stress field can be highly anisotropic, and compressive tangential stress can coexist with tensile radial stress at the interface between matrix and reinforcement.

Chevalier et al.[4] investigated the residual internal thermal stress in an $Al_2O_3$–$ZrO_2$ nanocomposite by X-rays and determined the compressive stress resulting in the $Al_2O_3$ matrix at $150 \pm 50$ MPa. The use of the Selsing equation yielded hydrostatic tension of 1.4 GPa in the $ZrO_2$ nanoparticles. In such nanocomposites, the $ZrO_2$ particles are well below the critical size for spontaneous phase transformation,[5] but also for transformation toughening.[6] Hence the only possible mechanism contributing to the toughness increase is the generation of residual stress. The intergranular nanoparticles situated at the grain boundaries, markedly strengthened the nanocomposite compared to the monolithic material. The high internal compressive stress acting on the alumina/alumina interfaces enhances the formation of a strong boundary structure decreasing the total probability of intergranular fracture. Therefore, the tensile residual micro-stresses that are expected at some grain boundaries of polycrystalline alumina because of thermo-elastic

* Corresponding author. Present address: Corning SAS, CETC, BP3- F-77210 Avon, France. Fax: +33 164 697454.
*E-mail address:* brunog@corning.com (G. Bruno).

0955-2219/$ – see front matter © 2008 Elsevier Ltd. All rights reserved.
doi:10.1016/j.jeurceramsoc.2007.12.037

anisotropy was reduced, These $Al_2O_3/ZrO_2$ nanocomposites showed a higher strength, fracture toughness ($K_{IC}$), threshold in the stress intensity factor under which no crack propagation occurs ($K_{I0}$) and lower wear rate than the monolithic alumina materials.[7] On the other hand, in "traditional" ZTA composites, when tetragonal $ZrO_2$ was incorporated into $Al_2O_3$ ceramics, due to the transformation toughening mechanisms, a significant increase in fracture toughness was observed.[8] The martensitic t → m (tetragonal to monoclinic) transformation in ZTA ceramics can be induced by applying a tensile stress. The applied stress required for the transformation is assisted by the internal residual stress in t-$ZrO_2$ particles. Micromechanics analyses predict that these residual stress vary as a function of the t-$ZrO_2$ content[9,10] and that the local stress field scales with the grain size.[11,12] It is therefore necessary to experimentally quantify the residual stresses in ZTA composites with various $ZrO_2$ content and different grain size.

Neutron diffraction is a well-established technique to tackle the problem of non-destructive determination of residual stress in bulk materials and components. Thanks to the high penetration of neutrons into matter, samples of several centimetres size can be probed. Moreover, multi-phase materials can be easily investigated, and the phase-specific stresses determined in parallel. Diffraction stress measurements basically consist of measuring the cell parameters of a material, or its interplanar spacing, and using the changes from unstressed values to obtain strain, then stress values. When a material is subject to a homogeneous strain field, the angular position of a diffraction peak will shift to lower or higher $2\theta$ values, depending on whether the strain is tensile or compressive. Residual stress in each phase can be deduced from the lattice strain by using basic linear elasticity. On the other hand, if the material is subjected to an inhomogeneous strain field, in addition to a possible shift in the peak position, the diffraction peak profile will also be broadened. Thus, while the shift of a peak measures the average lattice strain along a particular crystallographic direction, the peak width provides useful information about the distribution or fluctuation of the inhomogeneous (micro)-strain field. The technique is becoming a standard[13] for industrial quality assessment, especially for aerospace or nuclear applications. For some reason, however, its use on ceramic composites materials has been relatively limited. Majumdar et al.[14] reported some good examples of neutron diffraction on ceramic–ceramic composites. There are few detailed papers in the literature on neutron diffraction measurements of the residual stress in alumina–zirconia ceramic composites. Akiniwa et al.[15] measured the variation of residual stresses in ZTA composites with zirconia content from 15 to 75 vol%. Van Riessen et al.[16] observed the presence of both nonuniform and uniform strain effects in the ZTA composites by line-broadening estimations and cell parameters shifts, determined by Rietveld analysis. Sergo et al.[17] measured the residual stress in $Al_2O_3$/Ce–TZP (12 mol% $CeO_2$) sintered composites, containing 10, 20 and 40 vol% zirconia, and observed that the hydrostatic stress in the alumina phase varied linearly with zirconia content. In two companion papers, Wang et al.[18] and Alexander et al.[19] studied the internal stresses and the martensitic transformation in various $Al_2O_3$/Ce–TZP (also 12 mol% $CeO_2$) as a function of zirconia volume fraction. They used a powder diffractometer and consequently measured an average strain, therefore assumed to be hydrostatic. The obtained a linear dependence of the internal strains as a function of $ZrO_2$ volume fraction and stress values as high as 1 GPa for $ZrO_2$ and 100 MPa for $Al_2O_3$ (with 10 vol% $ZrO_2$). For ceramic nanocomposites, Todd et al.[20] measured the strain normal to the {0 0 6} and {3 0 0} planes by neutron diffraction and calculated that the addition of 5 wt.% SiC nanoparticles to alumina reduced the intergranular stresses by about 7%.

In this work the neutron diffraction determination of the residual stress in composites with alumina matrix containing different amount and nano- to micro-sized zirconia particles is reported. The influence of the microstructure on the residual stress is shown by comparing the present results to the literature quoted above.

## 2. Experimental

### 2.1. Sample preparation and microstructure

A high purity alumina powder α-$Al_2O_3$ >99.9 wt.% (Condea HPA 0.5, Ceralox division, Arizona, USA), with an average particle size of 0.45 μm, was mixed with 1.7 (A1.7Z), 14 (A14Z) and 22 (A22Z) vol% of yttria-stabilized zirconia powder (3Y-TZP, TZ-3YS, Tosoh Corp., Tokyo, Japan), with mean particle size of 0.26 μm. Different stable aqueous suspensions of 65 wt.% solids content using 0.5 wt.% addition of an alkali-free organic polyelectrolite (Dolapix C64) were obtained. Ball milling was then performed using high purity alumina balls in an alumina jar for 24 h. Plates (100 mm × 100 mm × 5 mm) were cast from each suspension in plaster of Paris mould and dried in air at room temperature for 48 h. Samples were then sintered at 1600 °C for 2 h in air. Sintered plates were then machined to small bars of 4 mm × 3 mm × 40 mm.

The microstructure of the sample was analyzed by SEM (scanning electron microscope) micrographs on polished samples, preliminarily thermally etched in air at 1450 °C for 30 min. The grain size of the alumina matrix was determined using the linear intercept method. For the measured of the $ZrO_2$ grain size distribution, micrographs were taken of representative regions and the equivalent spherical diameters of 100 grains were measured.

### 2.2. Neutron diffraction

Neutron diffraction residual stress analysis was carried out on the above-mentioned composite bars. Additionally, bars of monolithic alumina and zirconia processed in the same way as the composites and some corundum (α-alumina) powder (held in vanadium cans) with similar average grain size as the final composites were measured as a reference sample.

Measurements were done on the strain scanner (SALSA) at the Institute Laue-Langevin (ILL, Grenoble, France).[21,22] The 3 1 1 reflection of the double-focussing Si-monochromator was used at a take-off angle of 85° to obtain a wavelength of λ = 1.77 Å. A 2D position sensitive detector with an angu-

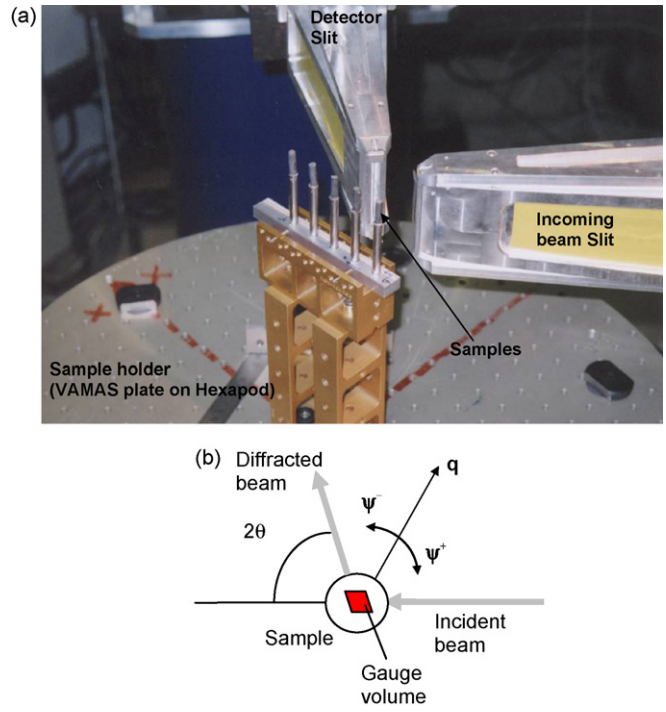


Fig. 1. (a) Photo of the SALSA set-up. The most important elements of the diffractometer are indicated and (b) sketch of the diffraction geometry with definition of the symbols quoted in the text.

lar opening of approximately 5° is typically mounted on SALSA. Primary and secondary slits defined a gauge volume of 1.5 mm × 1.5 mm × 10 mm. A photo of the sample mount on SALSA is shown in Fig. 1a. The lattice strains were measured for different orientations $\psi$ of the scattering vector **q** with respect to the sample main axes, in each sample (see sketch in Fig. 1b). This is called the $\sin^2\psi$ technique[23] and allows determining the full strain tensor. In our case its use gave us information about the deviatoric character of the strains. Typical counting times with this set-up varied from 5 to 30 min to account for the little $ZrO_2$ content (obviously, the smaller the reinforcement content, the weaker the diffraction signal). For $Al_2O_3$ the 1 1 9 reflection was selected that produces a Bragg peak at $2\theta \sim 89°$. For the $ZrO_2$, the (2 2 0) peak was chosen for strain scanning, at a diffraction angle $2\theta \sim 86°$. These peaks were chosen because they had a relatively high intensity and no overlap with other peaks. Moreover, as mentioned in,[24] the diffraction angle $2\theta \sim 90°$ satisfies a homogenous coverage of the gauge volume while rotating the sample. The LAMP software[25] was used to analyze the experimental results and obtain the peak parameters at each sample orientation.

The analysis flow can be schematised as:

1. The lattice elastic strain, as averaged within the gauge volume and in the direction of the scattering vector (sample tilt $\psi$), was obtained by:

$$\varepsilon_{hkl}^{\psi} = \frac{d_{hkl}^{\psi} - d_{hkl}^{0}}{d_{hkl}^{0}} = -\Delta\theta \cot\theta \tag{1}$$

where $d_{hkl}$ and $d_{hkl}^0$ are, respectively, the $h\,k\,l$ interplanar spacing of the sample and of the unstressed (reference). In our case monolithic $Al_2O_3$ bar was used as a reference, since this would allow discarding any macro-stress, although none is expected. For a monochromatic beam any change in lattice spacing will cause a corresponding shift $\Delta\theta$ in the angular position of the Bragg reflection, with respect to the reference $\theta$.

2. The strain was multiplied by the peak-specific appropriate elastic constant (Hooke's law) to obtain stresses. The samples were rotated in the scattering plane and measured around two perpendicular orientations (at three to four angular tilts). However, the average between each group of measurements was carried out: as it will be seen later, the strains in the normal and in-plane direction proved to be essentially equal and therefore could be considered hydrostatic.

   Therefore, bulk elastic constants could be used, and Hooke's law reads:

$$\sigma_i = \frac{E_{i,hkl}}{(1 - 2\nu_{i,hkl})}\varepsilon_{i,hkl} \tag{2}$$

   In Eq. (2) the strain and the elastic constants depend from the phase $i$ and the lattice plane ($h\,k\,l$) while the stress should not. In the present work, the elastic constants used were:

   for $Al_2O_3$: $E = 398$ GPa, $\nu = 0.23$

   for $ZrO_2$: $E = 226$ GPa, $\nu = 0.25$

3. The macro-stress could be calculated by the rule-of-mixtures

$$\sigma^M = \sum_i f_i \sigma_i \tag{3}$$

   where $f_i$ are the volume fractions of the component phases.

As it was mentioned before, in our case macro-stresses are supposed to be very small or vanishing, because of the production route. Therefore, the phase-specific stresses must satisfy the relation

$$f_{ZrO_2}\sigma_{ZrO_2} = (f_{ZrO_2} - 1)\sigma_{Al_2O_3} \tag{4}$$

Eq. (4) has been used as a cross check that the hypothesis of vanishing macro-stresses holds effectively. We will see below that the choice of the monolithic alumina as a reference was correct.

## 3. Results and discussion

### 3.1. Microstructure

The A1.7Z composite shows nano-sized $ZrO_2$ particles (300–600 nm) homogeneously distributed (Fig. 2a). In contrast, the A14Z and A22Z composites show larger $ZrO_2$ particles, less homogeneously distributed in the $Al_2O_3$ matrix. A significant amount of aggregates (up to ≈5 μm) are present (Fig. 2b and c).

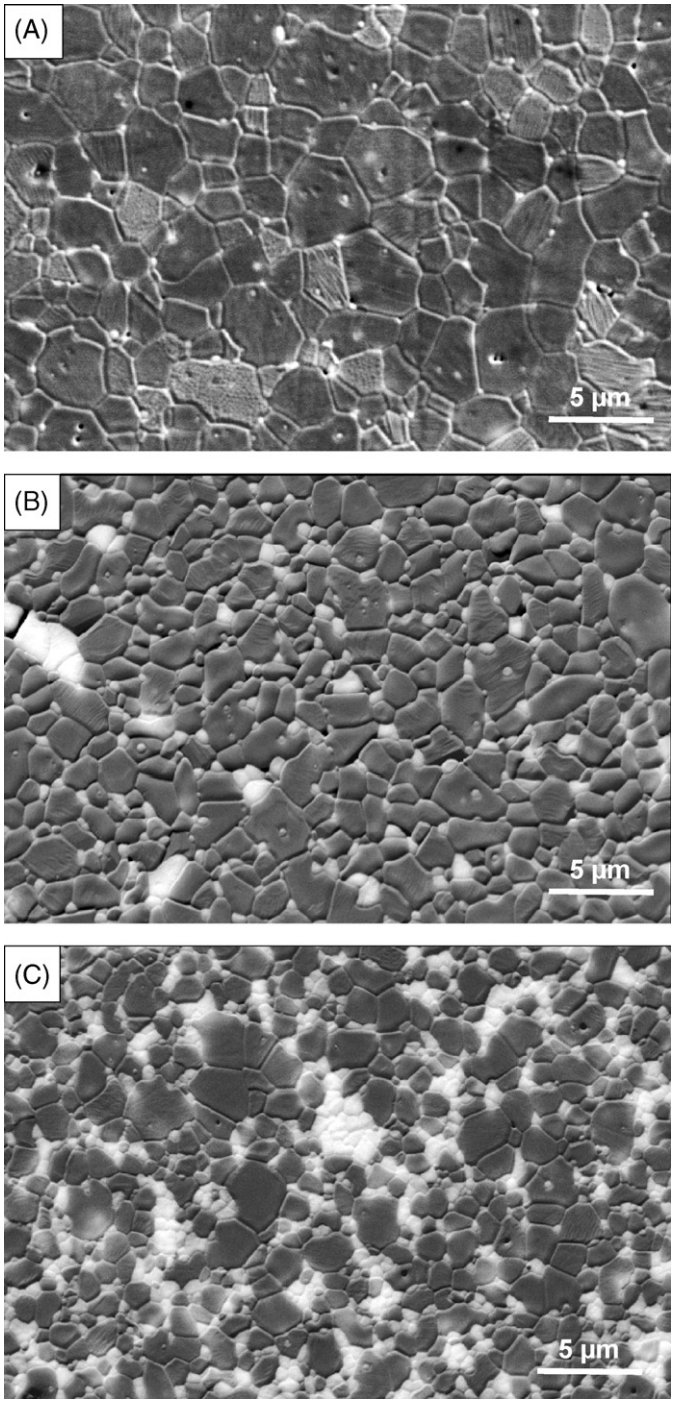


Fig. 2. Microstructure of the composites under investigation (SEM micrographs after thermal etching): (a) 1.7 vol% 3Y–TZP (A1.7Z); (b) 14 vol% 3Y–TZP (A14 Z); (c) 22 vol% 3Y–TZP (A22Z). White grains are zirconia particles, dark grains are alumina.

The mean grain size of the alumina matrix for A1.7Z, A14Z and A22Z composites are 3.8, 2.5 and 2 μm respectively.

### 3.2. Neutron diffraction analysis

The $\sin^2 \psi$ plots for the $ZrO_2$ phase of the various composites are shown in Fig. 3. It is clear that the strains are the same in the plane normal to the long sample axis. This is in good agreement

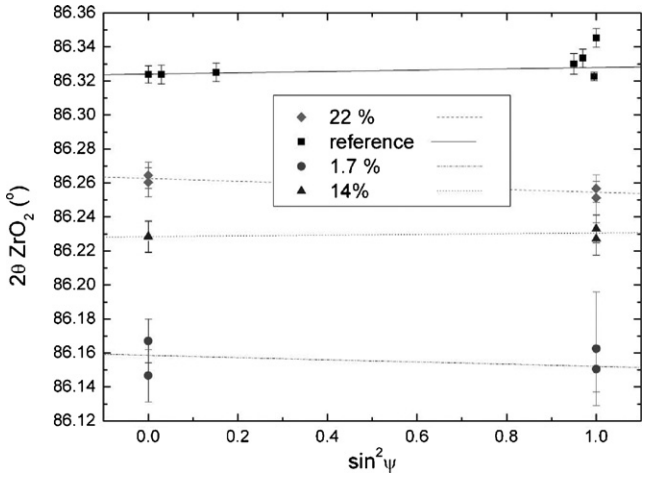


Fig. 3. $\mathrm{Sin}^2\ \psi$ plots for the $ZrO_2$ phase at different volume fractions.

with the findings of Ruiz-Hervias et al.[26] Hydrostatic stresses were found in even in a plane geometry.

For the A1.7Z composite, the $ZrO_2$ diffraction signal was always sufficient to reliably determine peak positions, even if the grain size was only about 300 nm (practically a nanocomposite). This nanocomposite displays a relatively large error bar, due to the poorer counting statistics. All $ZrO_2$-specific strains are tensile with respect to the reference and increase as the $ZrO_2$ content gets lower. The results of the strain calculations are given in Fig. 4. As expected, the $Al_2O_3$ matrix strain values increase monotonically with $ZrO_2$ concentration, which implies that the residual stress has indeed its origin in the thermal mismatch. This statement holds since no $t \rightarrow m$ transformation occurs in these materials, as documented in.[27] Moreover, if any transformation would occur, a discontinuity in the strain *vs*. $ZrO_2$ volume fraction behaviour would appear.

As shown in Fig. 4, the specific strain in both phases is roughly a linear function of the zirconia volume fraction.

The phase-specific (hydrostatic) stresses, as calculated by the method outlined in the previous section, are shown in Fig. 5. In agreement with the behaviour of the lattice strains, the calcu-

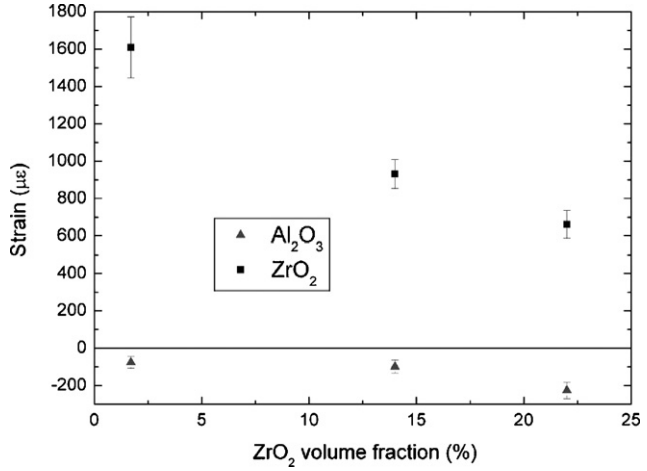


Fig. 4. Phase-specific strain for the alumina and the zirconia, as a function of the zirconia volume fraction.

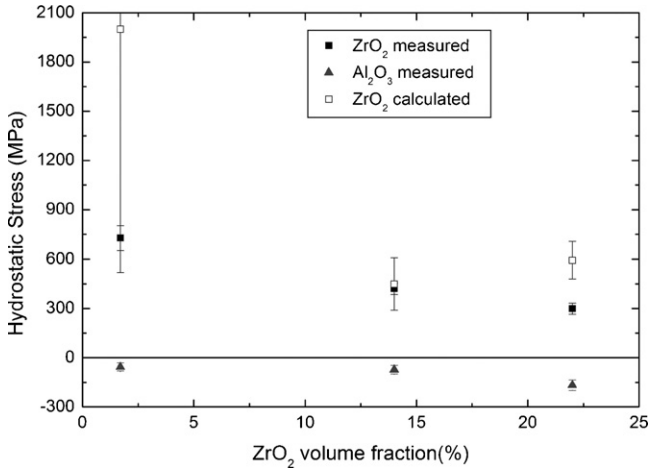


Fig. 5. Measured and calculated (via the macro-stress balance) phase-specific stress for the alumina and the zirconia, as a function of the zirconia volume fraction.

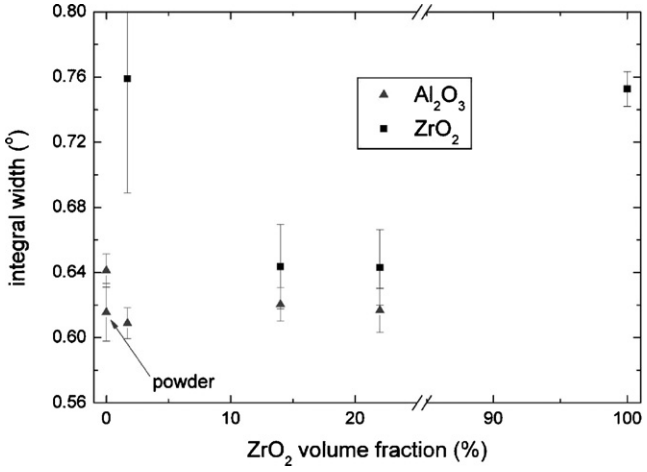


Fig. 6. Integral peak width for the alumina and the zirconia, as a function of the zirconia volume fraction.

lated hydrostatic stress in $ZrO_2$ particles is tensile and increases continuously as the $ZrO_2$ volume fraction decreases. For the $Al_2O_3$ matrix, the calculated hydrostatic stress is compressive and increases progressively with an increase in $ZrO_2$ volume fraction. This also conveys the message that the measured stress does satisfy the balance Eq. (4) -light symbols-, as the calculated and the experimental values are in very good agreement.

The last result is not as clear for the nanocomposite with 1.7 vol% $ZrO_2$, as it is for the others. It is to be noticed, however, that the alumina stress is very small for the 1.7 vol% $ZrO_2$ composites; therefore, a small error on the alumina stress value yields a very large error bar on the zirconia stress while applying Eq. (4), because of the small zirconia volume fraction. We can then state that the calculated value does agree with the measured data within the (large) error bar (which represents one standard deviation).

Moreover, these results are in qualitative agreement with previously reported data[4]: the measured value is a factor of 2 smaller, while the calculated value is about 40% bigger than the values determined in.[4] Those discrepancies can have two possible explanations:

(a) The reinforcement is located mainly at grain boundary (or even at triple points) in the present, while it is intragranular in Ref.[4]. This means that in the present materials stress relaxation can indeed take place, contrary to what happens in.[4] This would explain the reduction of stress in the present work.
(b) The literature data[4] were obtained by X-Ray, and therefore may suffer from surface effects (e.g. finishing), which would explain the even higher stresses determined by Chevalier et al.[4]

In addition, good qualitative agreement between the present work and the work of Wang et al.[18] holds, with again a reduction factor of about 2. In Ref.[18] stresses calculated by means of the balance Eq. (4) were lower than the measured values, while in the present they are in excess. Possibly, the different chemistry and microstructure causes the quantitative experimental discrepancies.

The substantial equivalence of the mean field stress of the different materials can be read from Fig. 6. This shows the peak integral width for the alumina 1 1 9 and the zirconia 2 2 0 reflections. For the alumina phase, the peak width varies little as a function of the $ZrO_2$ content and shows a similar value to the alumina powder. The monolithic alumina has a slightly higher peak width. As mentioned before, if a material is subjected to an inhomogeneous strain field the diffraction peak profile will also be broadened. In our measurements, a decrease of the $Al_2O_3$ peak width from the monolithic matrix shows that the stress state in the alumina matrix of these composites is possibly more homogeneous. This idea is coherent with the stress redistribution mechanism proposed above although the integral width difference is of the order of the error bar. This reduction in the intergranular stresses may influence the crack initiation and therefore, the mechanical properties of these materials. This result is more important in the A1.7Z nanocomposite, where the effect of the $ZrO_2$ nanoparticles should simply superpose to the intergranular tensile stresses of the alumina matrix. On the other hand, the alumina powder sample has slightly smaller peak width than the bulk monolithic polycrystalline sample that develops high intergranular stresses as a result of thermal anisotropy. Finally, the monolithic zirconia has a definitely larger peak width than the dispersed particles in the various composites, for the same reasons mentioned above.

## 4. Summary and conclusions

In summary, we have used neutron diffraction for the determination of the residual stress in ZTA ceramic composite containing different amount and grain size of $ZrO_2$ reinforced phase. Evidence was presented that the residual stress in these composites were primarily due to thermal expansion mismatch between $Al_2O_3$ and $ZrO_2$. As a result of this mismatch, the $Al_2O_3$ matrix is in compression and the $ZrO_2$ particles are in tension. From the experimental strain data, the residual stresses

in both phases were evaluated. It was found that the compressive residual stress in the $Al_2O_3$ matrix is ∼150 MPa for a sample containing 22 vol% $ZrO_2$. The phase-specific strain decrease approximately linearly with an increase in the volume fraction of that phase. The width of the microstrain distribution (i.e. the peak width) decreases from the monolithic alumina to the ZTA composites, indicating that the strain state in the matrix more hydrostatic.

Finally, the measurements showed that the presence of a narrow size distribution of nanoparticles in the ZTA composites with low (1.7 vol%) $ZrO_2$ content reduces more effectively the thermal expansion anisotropy of the matrix grains than the large zirconia agglomerated grains present in composites with higher amount of zirconia phase. This is a striking result, because the thermal stresses have a dramatic effect on the mechanical behaviour of alumina materials.

## Acknowledgments

This work was supported by EU under project reference FP6-515784-2, by the Spanish Ministry of Science and Technology under project number MAT2006-10249-C02-01 and by the "Dirección General de Universidades e Investigación de la Consejería de Educación y Ciencia de la Comunidad de Madrid" and CSIC under project reference 200660M042. J.F.B. has been supported by Ministry of Science and Technology and CSIC under the "Ramón y Cajal" Program co-financed by European Social Fund. Beam time was granted by ILL, Exp. No. 7-01-163.

## References

1. Fitzpatrick, M. E., Hutchings, M. T. and Withers, P. J., Separation of macroscopic, elastic mismatch and thermal expansion misfit stresses in metal matrix composite quenched plates from neutron diffraction measurements. *Acta Mater.*, 1997, **45**, 4867–4876.
2. Dutta, I., Sims, J. D. and Seigenthaler, D. M., An analytical study of residual-stress effects on uniaxial deformation of whisker reinforced metal-matrix composites. *Acta Metall. Mater.*, 1993, **41**, 885–908.
3. Shen, Y. L., Finot, M., Needleman, A. and Suresh, S., Effective plastic response of 2-phase composites. *Acta Metall. Mater.*, 1995, **43**, 1701–1722.
4. Chevalier, J., Deville, S., Fantozzi, G., Bartolomé, J. F., Pecharroman, C., Moya, J. S. *et al.*, Nano-structured ceramic oxides with a Slow Crack Growth resistance close to covalent materials. *Nano Lett.*, 2005, **5**, 1297–1301.
5. Heuer, A. H., Claussen, N., Kriven, W. M. and Rühle, M., Stability of tetragonal $ZrO_2$ particles in ceramic matrices. *J. Am. Ceram. Soc.*, 1982, **65**, 642–650.
6. De Aza, A. H., Chevalier, J., Fantozzi, G., Schehl, M. and Torrecillas, R., Slow-Crack-Growth behavior of zirconia-toughened alumina ceramics processed by different methods. *J. Am. Ceram. Soc.*, 2003, **86**, 115–120.
7. Bartolomé, J. F., De Aza, A. H., Martín, A., Pastor, J. Y., Llorca, J., Torrecillas, R. *et al.*, Alumina/zirconia micro/nanocomposites, a new material for biomedical applications with superior sliding wear resistance. *J. Am. Ceram. Soc*, 2007, **90**, 3177–3184.
8. Kelly, P. M. and Rose, L. R. F., The martensitic transformation in ceramics-its role in transformation toughening. *Prog. Mater. Sci.*, 2002, **47**, 463–557.
9. Mori, T. and Tanaka, K., Average stress in matrix and average energy of materials with misfitting inclusions. *Acta Metall.*, 1973, **21**, 571–574.
10. Taya, M., Hayashi, S., Kobayashi, A. S. and Yoon, H. S., Toughening of a particulate-reinforced ceramic-matrix composite by thermal residual stress. *J. Am. Ceram. Soc.*, 1990, **73**, 1382–1391.
11. Chiu, Y. P., On the stress field due to initial strains in a cuboid surrounded by an infinite elastic space. *J. Appl. Mech.*, 1970, **44**, 587–590.
12. Fu, Y. and Evans, A. G., Some effects of microcracks on the mechanical properties of brittle solids-I. Stress strain and relations. *Acta Metall.*, 1985, **33**, 1515–1523.
13. *ISO/TTA 3:2001(E), polycrystalline materials—Determination of residual stresses by neutron diffraction*. International Organization for Standardization, Case Postale 56, CH-211 Geneva 20, Switzerland, 2001.
14. Majumdar, S., Singh, J. P., Kupperman, D. and Krawitz, A. D., Application of neutron diffraction to measure residual strains in various engineering composite materials. *J. Eng. Mater. Tech.*, 1991, **113**, 51–59.
15. Akiniwa, Y., Tanaka, K., Minakawa, M. and Morii, Y., Neutron diffraction study of thermal residual stress in ceramic composites. *Mater. Sci. Res. Intern.*, 2000, **6**, 281–286.
16. Van Riessen, A. and O'Connor, B. H., Assessment of residual strain in zirconia-toughened alumina using neutron diffraction. *J. Am. Ceram. Soc.*, 1993, **76**, 2133–2135.
17. Sergo, V., Wang, X.-L., Clarke, D. R. and Becher, P. F., Residual stresses in alumina/ceria-stabilized zirconia composites. *J. Am. Ceram. Soc.*, 1995, **78**, 2213–2214.
18. Wang, X.-L., Hubbard, C. R., Alexander, K. B., Becher, P. F., Fernandez-Baca, J. A. and Spooner, S., Neutron diffraction measurements of the residual stress in $Al_2O_3$–$ZrO_2$ ($CeO_2$) ceramic composites. *J. Amer. Ceram. Soc.*, 1994, **77**, 1569–1575.
19. Alexander, K. B., Becher, P. F., Wang, X.-L. and Hsueh, C. H., Internal stress and martensite start temperature in alumina–zirconia composites: effects of composition and microstructure. *J. Am. Ceram. Soc.*, 1995, **78**, 291–296.
20. Todd, R. I., Bourke, M. A. M., Borsa, C. E. and Brook, R. J., Neutron diffraction measurements of residual stresses in alumina/SiC nanocomposites. *Acta Mater.*, 1997, **45**, 1791–1800.
21. Hughes, D. J., Bruno, G., Pirling, T. and Withers, P. J., First impressions on SALSA, the engineering beamline at the ILL. *Neutron News*, 2006, **17**, 28–32.
22. Pirling, T., Bruno, G. and Withers, P. J., SALSA, a new concept for strain mapping at the ILL. *Mater. Sci. Eng. A*, 2006, **437**, 139–144.
23. Hauk, V., ed., *Structural and residual stress analysis by nondestructive methods*. Elsevier, Amsterdam, 1997.
24. Webster, P. J., Spatial resolution and strain scanning. In *Measurement of residual and applied stress using neutron diffraction, NATO Series*, ed. M. J. Hutchings and A. D. Krawitz. Kluwer Academics, 1992, pp. 235–251.
25. http://www.ill.fr/data_treat/lamp/front.html.
26. Ruiz-Hervias, J., Bruno, G., Gurauskis, J., Sanchez-Herencia, A. J. and Baudin, C., Neutron diffraction investigation for possible anisotropy within monolithic $Al_2O_3$/Y-TZP composites fabricated by stacking together cast tapes. *Scripta Mater.*, 2006, **54**, 1133–1137.
27. Deville, S., Chevalier, J., Fantozzi, G., Bartolomé, J. F., Requena, J., Moya, J. S. *et al.*, *J. Eur. Cer. Soc.*, 2003, **23**, 2975–2982.